IMPLICIT DENSITY FUNCTIONALS FOR THE EXCHANGE-CORRELATION ENERGY: DESCRIPTION OF VAN DER WAALS BONDS

E. ENGEL AND A. FACCO BONETTI

Inst. für Theor. Physik, Univ. Frankfurt, D-60054 Frankfurt/Main, Germany

The energy surface of the Helium dimer, as a prototype of a van der Waals bond molecule, is investigated within the framework of density functional theory. For the exchange-correlation energy an implicit density functional, depending on the Kohn-Sham orbitals, is applied in which exchange is treated exactly, while correlation is approximated by the lowest order contribution obtained by Kohn-Sham perturbation theory. The resulting energy surface is in fair quantitative agreement with highly accurate empirical data over the complete range of internuclear separations, demonstrating that the concept of orbital-dependent functionals can provide a seamless description of dispersion forces. As selfconsistent calculations with implicit functionals on the basis of the optimized potential method are rather time-consuming, the correlation part of the exchange-correlation functional is evaluated perturbatively in the Helium dimer calculations. However, we also present an approximate scheme for the evaluation of the corresponding correlation potential.

1 Introduction

The description of dispersion forces is a long-standing problem in density functional theory (DFT)[1-9] (for an introduction to DFT, see Ref. 10). As these forces extend into regions of space with vanishing density, their correct representation is a critical test for any approximation to the exchange-correlation (xc) energy functional E_{xc}. While state-of-the-art generalized gradient approximations (GGA) improve atomic and molecular properties (see, e.g., Ref. 11) over the standard local density approximation (LDA), their semilocal structure nevertheless does not allow the reproduction of van der Waals (vdW) bonds.[12] In view of these difficulties, research in DFT has for some time concentrated on the prediction of the leading vdW-coefficient C_6 which is accessible via the polarizabilities obtained from the Kohn-Sham (KS) orbitals of the isolated systems (atoms, molecular components).[3-7,9] However, for actual applications it is not sufficient to just focus on the asymptotic C_6/R^6-attraction as it has been shown[12] that this force is not the only binding mechanism in vdW systems. This emphasizes the importance of a seamless DFT description of vdW forces which reproduces the complete energy surface

$$E_b(R) = E[X_2](R) - 2E[X] \tag{1}$$

of vdW molecules, rather than just its asymptotic behavior (in (1) $E[X]$ denotes the ground state energy of system X, and we have restricted ourselves to dimers for simplicity, with R being the internuclear separation).

Recently, three concepts for a seamless DFT treatment of the vdW interaction have been introduced,[6-8] all three relying on the adiabatic connection formula for E_{xc} together with some approximation for its crucial ingredient, the coupling-constant-dependent response function $\chi_\lambda(\mathbf{r}, \mathbf{r}', \omega)$. Kohn *et al*[6] decompose the Coulomb interaction into a short and a long range part, which leads to

a corresponding decomposition of E_{xc}. The long range component of E_{xc} is then represented in terms of the (retarded) response function of the entire system, which can be calculated via time-dependent DFT (using the LDA for the xc-kernel). This scheme yields a very accurate value for the C_6 of Helium.[6] On the other hand, the evaluation of the complete (molecular) $\chi_\lambda(\mathbf{r}, \mathbf{r}', \omega)$ is a rather demanding task and no consistent approximation for the short range part of E_{xc} is presently available, so that full scale applications to vdW-bond molecules have not been reported so far. Utilizing the random phase approximation (RPA) in the "Dyson equation" of time-dependent DFT, Dobson *et al*[8] express χ_λ via the noninteracting response function and the xc-kernel of the homogeneous electron gas, both evaluated with a nonlocal average density $\bar{n}(\mathbf{r}, \mathbf{r}')$. This concept has been successfully tested for two jellium metal slabs, attracting each other by dispersion forces.[8] It depends, however, on the particular choice of $\bar{n}(\mathbf{r}, \mathbf{r}')$. It is not clear whether this choice has to be adjusted to the specific structure of the system under consideration. In an alternative approach, Lein, Dobson and Gross[7] restrict themselves to first order in the "Dyson equation" of time-dependent DFT and approximate the xc-kernel by its static x-only limit. This scheme yields rather realistic values for the C_6 of light atoms, the energy surfaces of vdW-bond molecules, however, have not yet been examined.

A further route to a seamless DFT description is provided by the concept of implicit, i.e., orbital-dependent, xc-functionals. To date, in most applications of this scheme[13–15] the exact representation of the exchange energy E_x via the Fock term (evaluated with the KS orbitals ϕ_k) is combined with a conventional density functional for the correlation energy E_c. Unfortunately, such combinations exhibit the same deficiency in the long-range behavior of $E_b(R)$ as the standard density functionals. Recently, however, two systematic (i.e., universal and parameter-free) orbital-dependent approximations for E_c have been presented for use with the exact E_x. On the one hand, the random-phase-approximation (RPA) has been put forward for application to metallic systems.[16,17] On the other hand, a correlation functional based on KS perturbation theory, $E_c^{(2)}$,[18,19] has been introduced. It has been shown that $E_c^{(2)}$ approaches the asymptotic vdW limit[19] and yields C_6-values in reasonable quantitative agreement with experimental values for light atoms.[7,9] Here we apply the combination of the exact E_x and $E_c^{(2)}$ (called XC2-functional hereafter) to He_2.[20] Our results demonstrate that the XC2-approach contains the basic physics required to reproduce vdW bonds. However, as in conventional many-body approaches, higher order correlation corrections have to be taken into account for a fully quantitative description of noble gas dimers.

The xc-potential corresponding to orbital-dependent xc-functionals has to be evaluated by the optimized potential method (OPM).[21] This procedure is computationally less efficient than LDA or GGA calculations, so that a perturbative treatment of orbital-dependent functionals on LDA or GGA basis would be desirable. However, our results show that at least the exact E_x has to be included selfconsistently (via the OPM). At the same time they seem to justify a perturbative use of $E_c^{(2)}$. Nevertheless, we also discuss a first, simple approximation which should allow the selfconsistent application of $E_c^{(2)}$.

2 Theory

In this section we summarize the systematic derivation of orbital-dependent xc-functionals as well as their practical application via the OPM. To start with, let us for a moment assume that the multiplicative Kohn-Sham (KS) potential v_s, which establishes the auxiliary single-particle system with the same density as the interacting system of interest,[10] is known. Later we will discuss, how v_s can actually be obtained. This potential defines a noninteracting Hamiltonian,

$$\hat{H}_s = \hat{T} + \int d^3r \ \hat{n}(\mathbf{r}) v_s(\mathbf{r}) , \tag{2}$$

which induces a decomposition of the interacting Hamiltonian $\hat{H}$ into a single- and a two-particle part,

$$\hat{H} = \hat{H}_s + (\hat{H} - \hat{H}_s) . \tag{3}$$

From here a perturbation expansion of the ground state energy, and thus of E_{xc}, suggests itself.[19, 22] To first order in $\hat{H} - \hat{H}_s$ the Fock-term is obtained as the exact exchange contribution E_x,

$$E_x = -\frac{e^2}{2} \sum_{\epsilon_i, \epsilon_j \leq \epsilon_F} (ij||ji) \tag{4}$$

$$(ij||kl) = \int d^3r_1 \int d^3r_2 \ \frac{\phi_i^\dagger(\mathbf{r}_1)\phi_k(\mathbf{r}_1)\phi_j^\dagger(\mathbf{r}_2)\phi_l(\mathbf{r}_2)}{|\mathbf{r}_1 - \mathbf{r}_2|} , \tag{5}$$

where the ϕ_k denote the KS-orbitals,

$$\left\{ -\frac{\nabla^2}{2m} + v_s(\mathbf{r}) \right\} \phi_k(\mathbf{r}) = \epsilon_k \phi_k(\mathbf{r}),$$

and ϵ_F is the Fermi level. As the ϕ_k are themselves functionals of the density n, albeit implicit ones, E_x can be viewed as the orbital-dependent representation of the exact density functional for E_x. This E_x then defines the DFT correlation energy E_c via $E_c = E_{xc} - E_x$.

Before proceeding to the second order contribution let us briefly discuss the method which allows to evaluate the multiplicative potential $v_{xc}(\mathbf{r}) = \delta E_{xc}[n]/\delta n(\mathbf{r})$ corresponding to an orbital-dependent E_{xc}. Applying the chain rule for functional differentiation twice, the derivative $\delta/\delta n(\mathbf{r})$ can be replaced by derivatives with respect to the ϕ_k, which leads directly to the OPM-integral equation,[21, 22]

$$\int d^3r' \ \chi_s(\mathbf{r}, \mathbf{r}') \ v_{xc}(\mathbf{r}') = \Lambda_{xc}(\mathbf{r}) , \tag{6}$$

where

$$\chi_s(\mathbf{r}, \mathbf{r}') = \frac{\delta n(\mathbf{r})}{\delta v_s(\mathbf{r}')} = \sum_{\epsilon_k \leq \epsilon_F} \sum_{l \neq k} \frac{\phi_k^\dagger(\mathbf{r})\phi_l(\mathbf{r})\phi_l^\dagger(\mathbf{r}')\phi_k(\mathbf{r}')}{\epsilon_k - \epsilon_l} + \text{c.c.} \tag{7}$$

is the static KS response function and the inhomogeneity reads

$$\Lambda_{xc}(\mathbf{r}) = \sum_k \left\{ \int d^3r' \left[\sum_{l \neq k} \frac{\phi_k^\dagger(\mathbf{r})\phi_l(\mathbf{r})}{\epsilon_k - \epsilon_l} \phi_l^\dagger(\mathbf{r}') \frac{\delta E_{xc}}{\delta \phi_k^\dagger(\mathbf{r}')} + \text{c.c.} \right] + |\phi_k(\mathbf{r})|^2 \frac{\partial E_{xc}}{\partial \epsilon_k} \right\}. \quad (8)$$

To keep the discussion as general as possible we have here assumed that E_{xc} not only depends on the KS orbitals but also on the KS eigenvalues ϵ_k.

In contrast to the LDA and GGA the representation of E_x via the Fock term leads to an exact cancellation of the self-interaction. Correspondingly the asymptotic decay of v_x compensates the self-interaction potential of the outermost electron, $v_x(\mathbf{r}) \underset{|\mathbf{r}| \to \infty}{\sim} -e^2/|\mathbf{r}|$ (for finite systems). This property generates a Rydberg series of unoccupied states which allows the description of negative ions.[22]

Extending the perturbation expansion to second order $E_c^{(2)}$ is obtained as most simple correlation contribution. It consists of two terms, the first one having the same form as the second order Møller-Plesset expression (MP2) and the second one reflecting the difference between the exchange-only (x-only) OPM and the Hartree-Fock (HF) ground state energy (ΔHF),

$$E_c^{(2)} = E_c^{\text{MP2}} + E_c^{\Delta\text{HF}}, \quad (9)$$

$$E_c^{\text{MP2}} = \frac{e^4}{2} \sum_{\epsilon_i, \epsilon_j \leq \epsilon_F < \epsilon_k, \epsilon_l} \frac{(ij||kl)[(ij||kl) - (ij||lk)]}{\epsilon_i + \epsilon_j - \epsilon_k - \epsilon_l}, \quad (10)$$

$$E_c^{\Delta\text{HF}} = \sum_{\epsilon_i \leq \epsilon_F < \epsilon_l} \frac{1}{\epsilon_i - \epsilon_l} \left| \langle i|v_x|l \rangle + e^2 \sum_{\epsilon_j \leq \epsilon_F} (ij||jl) \right|^2, \quad (11)$$

$$\langle i|v_x|l \rangle = \int d^3r \, \phi_i^\dagger(\mathbf{r})\phi_l(\mathbf{r})v_x(\mathbf{r}). \quad (12)$$

At this point unfortunately a problem arises: The direct application of the OPM, Eqs. (6-8), to $E_c^{(2)}$ leads to an asymptotically divergent potential.[23] This can be gleaned from the fact that for large $|\mathbf{r}|$ the response function on the left hand side of Eq. (6) is dominated by the most weakly bound occupied orbital. In contrast, the right hand side decreases much more slowly due to the appearence of excited states in (9). To circumvent this difficulty we recast $E_c^{(2)}$ in a different form which suggests an approximation for the correlation potential. For simplicity, we neglect $E_c^{\Delta\text{HF}}$ at this point, which seems legitimate in view of the fact that this term represents only a minor correction to the dominating E_c^{MP2}.[22] We then focus on the pair-correlation energies,

$$e_{ij}^{\text{MP2}} = \frac{e^4}{2} \sum_{\epsilon_F < \epsilon_k, \epsilon_l} \frac{(ij||kl)[(kl||ij) - (kl||ji)]}{\epsilon_i + \epsilon_j - \epsilon_k - \epsilon_l}. \quad (13)$$

The excited states in e_{ij}^{MP2} can be eliminated by a closure approximation (CA), assuming the individual eigenvalue differences in the denominator of (13) to be well

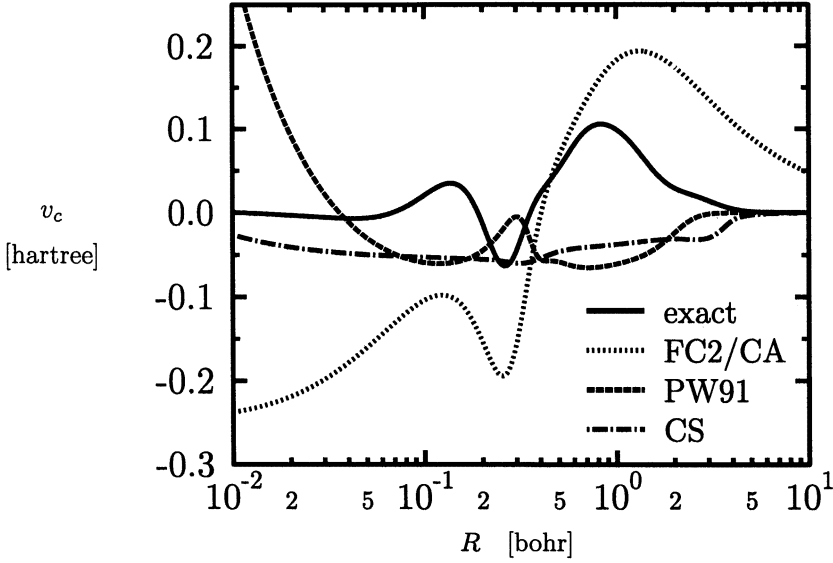Figure 1. Correlation potential of Ne: Exact v_c[24] versus PW91-GGA[25] and Colle-Salvetti (CS)[26] result as well as the closure approximated second order potential, $v_c^{(CA)}$.

represented by some average $\Delta\epsilon$,

$$
e_{ij}^{CA} = \frac{e^4}{2}\frac{1}{\Delta\epsilon}\bigg\{ (ij|||ij) - \sum_{\epsilon_k,\epsilon_l \le \epsilon_F} (ij||kl)(kl||ij)
$$
$$
- (ij|||ji) + \sum_{\epsilon_k,\epsilon_l \le \epsilon_F} (ij||kl)(kl||ji) \bigg\} \tag{14}
$$

$$
(ij|||kl) = \int d^3 r_1 \int d^3 r_2 \; \frac{\phi_i^\dagger(\mathbf{r}_1)\phi_k(\mathbf{r}_1)\phi_j^\dagger(\mathbf{r}_2)\phi_l(\mathbf{r}_2)}{|\mathbf{r}_1 - \mathbf{r}_2|^2}. \tag{15}
$$

e_{ij}^{CA} then allows to rewrite E_c^{MP2} as

$$
E_c^{MP2} = \sum_{\epsilon_i,\epsilon_j \le \epsilon_F} w_{ij}\, e_{ij}^{CA} \quad \text{with} \quad w_{ij} = e_{ij}^{MP2}/e_{ij}^{CA} \tag{16}
$$

(note that the arbitrary energy scale $\Delta\epsilon$ drops out of E_c^{MP2}). Until now, E_c^{MP2} has only been reformulated in an exact manner. However, understanding the w_{ij} as fixed numbers, rather than as functionals of ϕ_k and ϵ_k, a finite correlation potential $v_c^{(CA)}$ can be directly obtained by solving the OPM equation (6), varying only the e_{ij}^{CA}, Eq. (14). The result of this procedure is shown in Fig. 1 for the case of Ne, in comparison with the exact v_c,[24] the PW91-GGA[25] and the orbital-dependent Colle-Salvetti potential[26] (all approximations have been evaluated with the exact KS orbitals). Clearly, neither the GGA nor the semiempirical Colle-Salvetti approximation reproduces the orbital structure of the correct v_c. On the other hand,

$v_c^{(CA)}$ is the first DFT potential which at least qualitatively follows the exact v_c. Fig. 1 can thus be interpreted as an encouraging result, pointing at the systematic origin of $E_c^{(2)}$.

3   Dispersion forces

One can immediately demonstrate that the correlation functional (9) in principle reproduces the $1/R^6$-behavior of long-range dispersion forces. Consider two neutral, closed-subshell atoms A and B at very large internuclear separation R. The overlap between an occupied atomic KS-orbital of atom A, $\phi_{i,A}$, and an unoccupied orbital of atom B, $\phi_{l,B}$, then vanishes exponentially with increasing R (and vice versa). Consequently, the sums over KS states in Eqs. (10,11) can be decomposed with respect to the two centers A and B, $\sum_{\epsilon_i} \longrightarrow \sum_{\epsilon_{i_A}} + \sum_{\epsilon_{i_B}}$ (for homonuclear systems the degenerate symmetric and antisymmetric molecular orbitals have to be combined to localized atomic orbitals). The complete $E_c^{(2)}$ then splits into two R-independent terms, the atomic $E_c^{(2)}$ of the individual atoms, and an interaction component $E_{c,int}^{(2)}$,

$$E_{c,int}^{(2)} = e^4 \sum_{\epsilon_{i_A} \leq \epsilon_F < \epsilon_{k_A}} \sum_{\epsilon_{j_B} \leq \epsilon_F < \epsilon_{l_B}} \frac{(i_A j_B \| k_A l_B)(k_A l_B \| i_A j_B)}{\epsilon_{i_A} + \epsilon_{j_B} - \epsilon_{k_A} - \epsilon_{l_B}}. \tag{17}$$

Finally, after an expansion in powers of $1/R$, $E_{c,int}^{(2)}$ can be rewritten in a more familiar form,[1]

$$E_{c,int}^{(2)} = -\frac{C_6}{R^6} + \mathcal{O}(R^{-8}) \tag{18}$$

$$C_6 = \int_0^\infty \frac{du}{2\pi} \sum_{ijkl} \left(\delta_{ij} - 3\frac{R^i R^j}{R^2} \right) \left(\delta_{kl} - 3\frac{R^k R^l}{R^2} \right) \alpha_{A,ik}(iu) \alpha_{B,jl}(iu), \tag{19}$$

where α_{ik} denotes the atomic KS polarizability tensor,

$$\alpha_{ik}(\omega) = \int d^3 r_1 \int d^3 r_2 \; r_{1,i} \; r_{2,k} \; \chi_s^R(\mathbf{r}_1, \mathbf{r}_2, \omega), \tag{20}$$

which contains the atomic retarded KS response function χ_s^R. On the other hand, the electrostatic and exchange contributions to the interaction energy between A and B vanish exponentially with R for closed-subshell atoms, so that $E_{c,int}^{(2)}$ dominates $E_b(R)$ in the large-R regime. The functional (9) thus yields the correct asymptotic $1/R^6$-behavior of $E_b(R)$. The resulting van der Waals coefficient (19), on the other hand, differs from the full C_6 due to the fact that the KS polarizability (20) is not identical with the true one (cf. Ref. 7). However, these differences are of the order of 10-20% for light atoms,[7,9] so that (9) appears to be a reasonable starting point for the DFT description of van der Waals bond molecules.

4   Technical details of the He-dimer calculations

The direct numerical solution of the OPM integral equation (6) is a rather time-consuming procedure even for the exchange functional (4) (cf. Refs. 13, 15, 27, 28).

We have thus used the Krieger-Li-Iafrate (KLI) approximation[29] for the solution of (6) which has been shown to give extremely accurate v_x for few electron atoms (see, e.g., Ref. 27). In particular, it is exact for Helium-like two-electron systems. In the following we will thus identify the KLI approximation with the full OPM for simplicity. Moreover, as mentioned in Section 2, a straightforward solution of (6) for the functional (9) does not seem to exist. While the closure approximation (16) might pave a way to the selfconsistent use of functionals like (9), its present form overestimates the true atomic correlation potential substantially. Moreover, even the application of the approximation (16) is computationally very demanding as the e_{ij}^{MP2} have to be evaluated for each iteration of the selfconsistency cycle. $E_c^{(2)}$ has thus been applied perturbatively in the calculations for the Helium dimer.

For the solution of the two-center Kohn-Sham equations we have used prolate spheroidal coordinates ξ, η, φ,

$$\xi = (r_1 + r_2)/R, \quad \eta = (r_1 - r_2)/R, \quad \varphi = \tan(y/x)$$
$$1 \leq \xi < \infty, \qquad -1 \leq \eta \leq 1 \qquad 0 \leq \varphi \leq 2\pi \tag{21}$$

where r_1, r_2 are the distances between the electronic position $\mathbf{r}$ and the two nuclei at the positions $(0, 0, \pm R/2)$. Due to the rotational symmetry with respect to the internuclear axis the KS orbitals can be classified as

$$\phi_i(\mathbf{r}) = \psi_{k,|m|}(\xi, \eta)e^{im\varphi}\chi_\sigma \quad , \quad m = 0, \pm 1, \pm 2, \ldots , \quad k = 1, 2, \ldots , \tag{22}$$

with χ_σ denoting the standard Pauli spinors. The cylindrical functions $\psi_{k,|m|}(\xi, \eta)$ are then expanded in terms of a nonorthogonal Hylleraas basis,[30]

$$\psi_{k,|m|}(\xi, \eta) = \sum_{n=0}^{n_{max}} \sum_{l=|m|}^{l_{max}+|m|} c_{nl|m|}^k P_l^{|m|}(\eta)(\xi^2 - 1)^{|m|/2}$$
$$\times \exp\left(-\frac{\xi - 1}{2a}\right) L_n^{|m|}\left(\frac{\xi - 1}{a}\right) , \tag{23}$$

where the L_n^m and P_l^m are generalized Laguerre polynomials and associated Legendre functions, respectively, and a is an adjustable parameter. The computational details can be found in Ref. 20 where also an extensive discussion of the accuracy of the results is given: The basis set and grid sizes as well as the parameter a have been chosen so that for the energy surface of He_2 an overall accuracy of better than 1μhartree is reached (without any extrapolation as e.g., to $l_{max} = \infty$).

5 Results

Our results for He_2 are given in Figs.2,3. Fig. 2 shows $E_b(R)$ for three DFT variants in comparison with HF[31] and essentially exact empirical results.[32] Similar to the HF approach, the x-only OPM (utilizing the exact exchange (4), but neglecting correlation completely) produces a strictly repulsive $E_b(R)$. Both energy surfaces are very close together, with the HF energy always being somewhat lower than the x-only OPM energy. This reflects the fact that, while the functional forms of the x-only OPM and HF energy are identical, the multiplicative OPM potential reduces the variational freedom marginally compared to the nonlocal HF potential
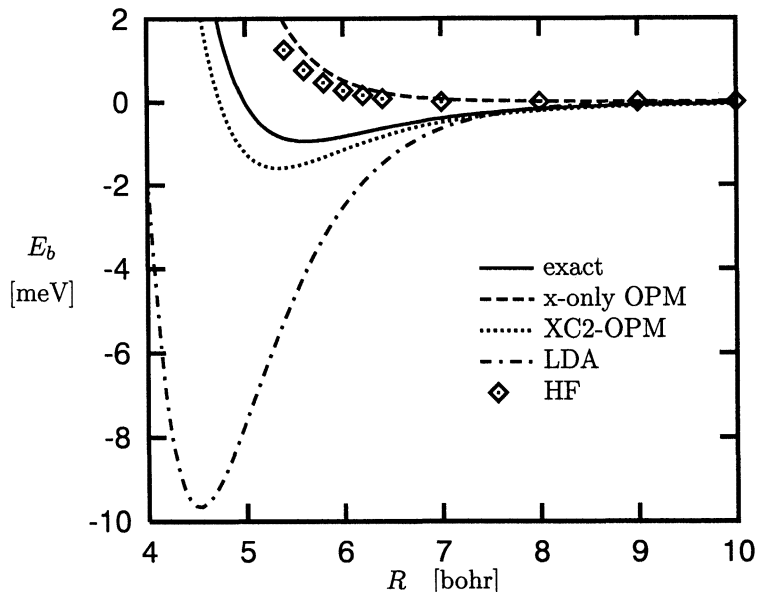
Figure 2. Energy surface of He$_2$: X-only and correlated OPM data versus LDA, HF[31] and exact[32] results.

in the case of He$_2$ (for atomic Helium the ground state energy of the x-only OPM is identical with the HF ground state energy). Note that the excellent agreement between the HF and x-only OPM results also corroborates the high accuracy of the KLI approximation for v_x in the case of He$_2$.

Turning to the LDA,[33] one recognizes that a bound Helium dimer is predicted, however, at an equilibrium separation R_e of 4.5 bohr and with an extremely large well depth D_e of 9.7 meV (all our LDA results are in good agreement with those of Ref. 12). The LDA needs a substantial overlap of the two atomic densities in order to generate an attractive force, and this overlap can only be achieved by bringing the atoms much closer together than they are in reality. This result reflects the general perception that the LDA is not suitable for describing vdW bonds.

Finally, inclusion of $E_c^{(2)}$ in the OPM scheme (abbreviated by XC2-OPM) leads to an energy surface in reasonable agreement with the exact $E_b(R)$: The XC2-OPM yields an R_e of 5.33 bohr and a D_e of 1.62 meV (exact: $R_e = 5.61$ bohr, $D_e = 0.95$ meV) which reduces the errors in both quantities by almost an order of magnitude compared to the LDA. As to be expected from the discussion of section 3, the XC2 energy surface shows the $1/R^6$-behavior for large R. The value for C_6 which is extracted from our numerical $E_b(R)$ under the assumption that for $R = 10$ bohr, $E_b(R) \equiv -C_6/R^6$ is 2.26 hartree bohr^6. This result deviates by only 0.6 hartree bohr^6 from the C_6 of 1.66 hartree bohr^6 obtained via (19) from the atomic KS polarizability of Helium,[7,9] consistent with our error estimate of better than 1 μhartree for the numerical $E_b(R)$.

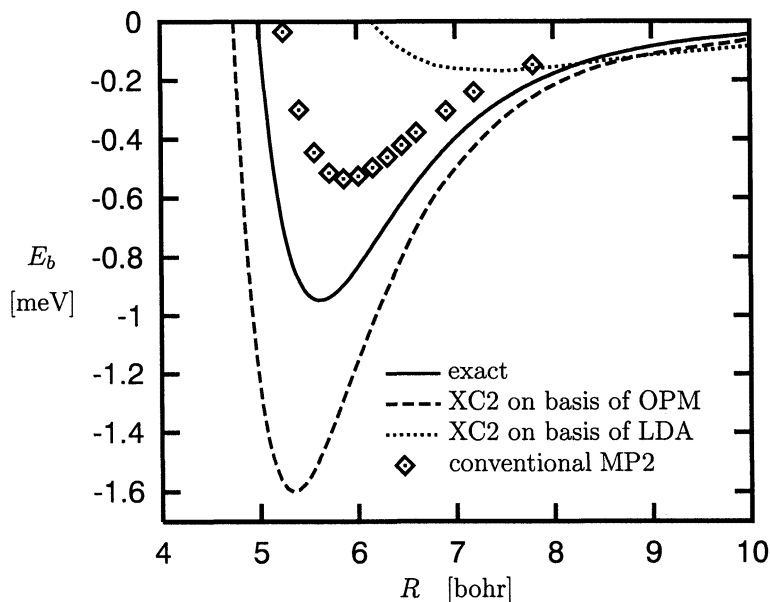Given the fact that the basic concept underlying the XC2-functional is second

Figure 3. Comparison of different second order perturbative approaches to the energy surface of He₂: Perturbative evaluation of the XC2-functional on the basis of the x-only OPM and LDA Hamiltonians versus conventional MP2 result.[34]

order perturbation theory the realistic $E_b(R)$ obtained with the XC2-OPM might not be surprising. Clearly, the functional (9) will lead to an asymptotic $1/R^6$-dependence, irrespectively of the type of the single-particle orbitals used in (9): The specific nature of the ϕ_k is not used for the derivation of (18). However, this does not imply that the resulting $E_b(R)$ reproduces the exact energy surface for any choice of the single-particle Hamiltonian. This is demonstrated in Fig. 3 where we compare three variants of second order perturbation theory. In addition to the XC2-OPM we plot the $E_b(R)$ obtained by a second order expansion using selfconsistent LDA orbitals (XC2-LDA) and the conventional second order Møller-Plesset (MP2) result[34] (based on the HF Hamiltonian). In the case of the XC2-LDA $E_c^{\Delta HF}$ involves the difference between the nonlocal HF exchange and the LDA xc-potential, and the Fock expression for E_x is also evaluated with LDA orbitals. The spectroscopic constants found with the XC2-LDA ($R_e = 7.44$ bohr, $D_e = 0.17$ meV) are rather different from the XC2-OPM values. In spite of these large deviations, however, the XC2-LDA produces a $1/R^6$ tail in $E_b(R)$ with a value for C_6 which is only 30% larger than the C_6 calculated with the XC2-OPM. The MP2 scheme, on the other hand, overestimates R_e as much ($R_e = 5.88$ bohr) as the XC2-OPM underestimates it. Accordingly, the MP2 underestimates D_e by about 35% ($D_e = 0.53$ meV), while the XC2-OPM overestimates it by 50%. These results demonstrate that second order perturbation theory does not automatically generate a realistic $E_b(R)$, i.e., independently of the underlying zeroth order Hamiltonian. The HF Hamiltonian and the x-only OPM Hamiltonian bracket the exact result,

so that they appear to be equally suitable as starting point for a perturbation expansion. In both cases, however, higher order correlation corrections are required to obtain a complete quantitative agreement with the exact $E_b(R)$ (cf. Ref. 34). It remains to be examined to what extent a suitable selfconsistent treatment of the functional (9) changes this picture.

In order to understand the differences between the XC2-OPM, XC2-LDA and MP2 energy surfaces one has to analyze the underlying single-particle spectra. First of all, one finds quite generally that the value for E_c^{MP2} obtained with LDA states is larger than that calculated from OPM states, which, in turn, is larger than the conventional MP2 correlation energy (see Ref. 22). This relative size is, on the one hand, controlled by the eigenvalue gap between the highest occupied (HOMO) and the lowest unoccupied (LUMO) orbitals: This gap is smaller in the case of the OPM ($\epsilon^{HOMO} = -916$ mhartree, $\epsilon^{LUMO} = -172$ mhartree at $R = 5.8$ bohr) than for the HF approach, for which ϵ^{HOMO} is essentially identical, but $\epsilon^{LUMO} = 0$. The gap is still smaller for the LDA spectrum ($\epsilon^{HOMO} = -572$ mhartree, $\epsilon^{LUMO} = +19$ mhartree for our basis). As a consequence, the XC2-OPM value for E_c^{MP2} is 20% larger than the MP2 result. An analogous difference shows up for atomic Helium and, finally, in $E_b(R)$. On the other hand, while the XC2-LDA value for E_c^{MP2} is still larger than the XC2-OPM result, the difference amounts to only 2%, compared with the 23% increase of the gap. This clearly shows that not only the size of the gap, but also the form of the orbitals entering the Slater integrals in (9) is important for the final value of E_c^{MP2}. Nevertheless, with E_c^{MP2} being larger in the case of the XC2-LDA, one might expect that the resulting $E_b(R)$ is more attractive than the XC2-OPM result. However, a significant error is introduced into the XC2 ground state energy by the perturbative evaluation of the comparatively large E_x, Eq. (4), with LDA orbitals. While the correction (11) compensates most of this error, the net effect is a XC2-LDA ground state energy which is 1.90 mhartree less attractive (again for $R = 5.8$ bohr) than its XC2-OPM counterpart. Upon subtraction of the atomic ground state energy one ends up with a completely different $E_b(R)$, indicating the extreme sensitivity of the He$_2$ energy surface to the accurate handling of the exchange functional: E_x must be treated selfconsistently in order to obtain a realistic $E_b(R)$ for He$_2$ with the XC2-functional.

Acknowledgments

References

1. E. Zaremba and W. Kohn, *Phys. Rev.* B **13**, 2270 (1976).
2. K. Rapcewicz and N. W. Ashcroft, *Phys. Rev.* B **44**, 4032 (1991).
3. S. J. A. Gisbergen, J. G. Snijders, and E. J. Baerends, *J. Chem. Phys.* **103**, 9347 (1995); V. P. Osinga, S. J. A. Gisbergen, J. G. Snijders, and E. J. Baerends, *J. Chem. Phys.* **106**, 5091 (1997).

4. Y. Andersson, D. C. Langreth, and B. I. Lundqvist, *Phys. Rev. Lett.* **76**, 102 (1996); E. Hult, Y. Andersson, B. I. Lundqvist, and D. C. Langreth, *Phys. Rev. Lett.* **77**, 2029 (1996).
5. J. F. Dobson and B. P. Dinte, *Phys. Rev. Lett.* **76**, 1780 (1996).
6. W. Kohn, Y. Meir, and D. E. Makarov, *Phys. Rev. Lett.* **80**, 4153 (1998).
7. M. Lein, J. F. Dobson, and E. K. U. Gross, *J. Comput. Chem.* **20**, 12 (1999).
8. J. F. Dobson and J. Wang, *Phys. Rev. Lett.* **82**, 2123 (1999); J. F. Dobson, B. P. Dinte, and J. Wang, in *Electronic Density Functional Theory: Recent Progress and New Directions*, eds. J. F. Dobson, G. Vignale, and M. P. Das (Plenum, New York, 1998), p. 261.
9. A. Görling, H. H. Heinze, and M. Levy, *Phys. Rev. A*, in press.
10. R. M. Dreizler and E. K. U. Gross, *Density Functional Theory*, (Springer, Berlin, 1990).
11. B. G. Johnson, P. M. W. Gill, and J. A. Pople, *J. Chem. Phys.* **98**, 5612 (1993).
12. D. C. Patton and M. R. Pederson, *Phys. Rev. A* **56**, R2495 (1997).
13. T. Kotani, *Phys. Rev. Lett.* **74**, 2989 (1995).
14. D. M. Bylander and L. Kleinman, *Phys. Rev. Lett.* **74**, 3660 (1995); and *Phys. Rev. B* **55**, 9432 (1997).
15. M. Städele, J. A. Majewski, P. Vogl, and A. Görling, *Phys. Rev. Lett.* **79**, 2089 (1997).
16. T. Kotani and H. Akai, *J. Magn. Magn. Mater.* **177-181**, 569 (1998).
17. E. Engel and A. Facco Bonetti, in *Quantum Systems in Theoretical Chemistry and Physics, Vol.1: Basic Problems and Model Systems*, ed. by A. Hernández Laguna et al. (Kluwer, Dordrecht, 2000) p.227.
18. A. Görling and M. Levy, *Phys. Rev. A* **50**, 196 (1994).
19. E. Engel, A. Facco Bonetti, S. Keller, I. Andrejkovics, and R. M. Dreizler, *Phys. Rev. A* **58**, 964 (1998).
20. E. Engel, A. Höck, and R. M. Dreizler, *Phys. Rev. A*, in press.
21. J. D. Talman and W. F. Shadwick, *Phys. Rev. A* **14**, 36 (1976).
22. E. Engel and R. M. Dreizler, *J. Comput. Chem.* **20**, 31 (1999).
23. A. Facco Bonetti and E. Engel, unpublished (1999).
24. C. J. Umrigar, private communication (1995); C. Filippi, X. Gonze, and C. J. Umrigar, in *Recent Developments and Applications in Density Functional Theory*, ed. by J. Seminario (Elsevier, Amsterdam, 1996).
25. J. P. Perdew, in *Electronic Structure of Solids 1991*, eds. P. Ziesche and H. Eschrig (Akademie Verlag, Berlin, 1991), p.11.
26. R. Colle and O. Salvetti, *Theoret. Chim. Acta* **37**, 329 (1975).
27. J. B. Krieger, Y. Li and G. J. Iafrate, *Phys. Rev. A* **45**, 101 (1992).
28. E. Engel and S. H. Vosko, *Phys. Rev. A* **47**, 2800 (1993).
29. J. B. Krieger, Y. Li, and G. J. Iafrate, *Phys. Lett. A* **146**, 256 (1990).
30. E. A. Hylleraas, *Z. Phys.* **71**, 739 (1931).
31. D. M. Silver, *Phys. Rev. A* **21**, 1106 (1980).
32. R. A. Aziz and M. J. Slaman, *J. Chem. Phys.* **94**, 8047 (1991).
33. For the LDA correlation potential the parametrization of S. H. Vosko, L. Wilk, and M. Nusair, *Can. J. Phys.* **58**, 1200 (1980), has been used.
34. D. E. Woon, *J. Chem. Phys.* **100**, 2838 (1994).